2. S. J. Young, "Nonisothermal band model theory," J. Quant. Spectr. Rad. Trans., 18, No. 1A, 1-28 (1977).
3. A. R. Curtis, "Discussion of 'A statistical model for water-vapor absorption' by R. M. Goody," Q. J. R. Meteorol. Soc., 78, No. 338, 638-640 (1952).
4. W. L. Goodson, "The evaluation of infrared radiative fluxes due to atmospherical water vapor," Q. J. R. Meteorol. Soc., 79, No. 341, 367-379 (1953).
5. Yu. V. Khodyko, É. I. Vitkin, and V. P. Kabashnikov, "Methods of computing molecular gas radiation on the basis of modeling spectral composition," Inzh.-Fiz. Zh., 36, No. 2, 204-217 (1979).
6. S. S. Penner, Quantitative Molecular Spectroscopy and Gas Emissivities, Addison-Wesley (1959).
7. L. D. Landau and E. M. Lifshits, Quantum Mechanics, Pergamon (1977).

THEORETICAL MODEL OF HIGH-CURRENT RELATIVISTIC ELECTRON-BEAM INTERACTION WITH A METAL OBSTACLE

G. S. Romanov, M. V. Suzdenkov, A. V. Teterev, and F. G. Fokov

UDC 536.422.1

A method is described and results are presented for a numerical computation of crater and plasma-flare formation under the effect of a high-current relativistic electron beam on an aluminum obstacle.

During the interaction of high-current charged-particle beams, for example, relativistic electron beams (REB), withhigh power density and a metal obstacle, heating, evaporation, and rupture occur. The set of physical processes governing the dynamics of crater formation and the ejection of mass in the form of highly ionized target vapors differs substantially here from the sufficiently well-studied processes accompanying material treatment by particle beams at moderate energy-flux densities [1, 2]. Computations and experiments [2-4] show that for 10^6-10^7-A beam currents and 1-10-MeV electron energies the pressure in the action domain reaches 1-50 Mbar, the temperature 10-30 eV, and the velocity of the vapors being ejected 100 km/sec. A hydrodynamic model in which dissipative processes associated with charged-particle beam energy transfer to the target substance, target deformation and rupture under the effect of the shockwave, and energy transfer in the highly heated target vapors by the radiation diffusion mechanism are taken into account is applicable for the description of the dynamics of phenomena with such parameters.

Such a model is considered in this paper. It is here taken into account that the motion that occurs is axisymmetric and the target can be both finite and semiinfinite in thickness. We mention that in an analogous formulation, but without the spatial distribution of the energy liberation zone and the radiation diffusion of the energy in the vapor flare taken into account, the described problem was solved numerically in [4]; however, the results presented there do not afford the possibility of composing a sufficiently complete representation of the parameters of the motion that occurs.

Let us consider formulation of the problem. Energy is liberated in a certain volume of the target because of REB action, resulting in melting, evaporation, and ionization of the target material. Under the action of pressure forces the substance is set in motion, a plasma flare is formed, and a crater in the target. Since REB with electron energies above 0.1 MeV produce an interaction zone with quite definite volume nature in the target, we apply the method of multiple electron scattering in a substance to compute the zone by using angular distributions computed by Goudsmit-Sanderson theory. Preliminary computations of the energy liberation zone configuration in the 0.5-10-MeV electron energy range displayed good agreement with the results of computations by the successive collisions model [6], as well as with the experimental results [4, 6]. The density profiles in the interaction zone vary during the

Scientific-Research Institute of Applied Physical Problems. V. I. Lenin Belorussian State University, Minsk. Translated from Inzhenerno-Fizicheskii Zhurnal, Vol. 47, No. 6, pp. 952-957, December, 1984. Original article submitted July 21, 1983.

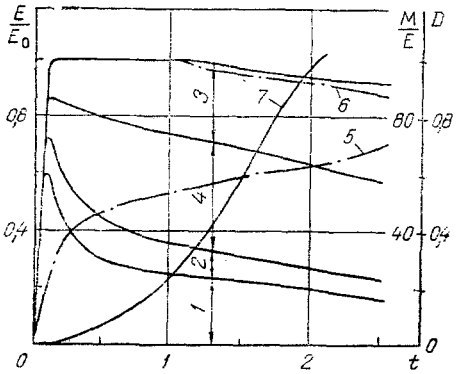

Fig. 1

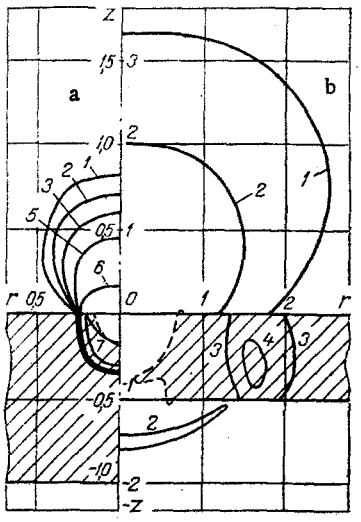

Fig. 2

Fig. 1. Integral characteristics of REB interaction with a target: 1) thermal; 2) kinetic energy in the target; 3) thermal; 4) kinetic energy in the vapor flare; 5) growth of crater depth; 6) growth of hole from rear side of the target; 7) specific mass ejection M/E, μg/J; D, cm; t, μsec.

Fig. 2. Isobars of the interaction process: a) t = 0.115 μsec; b) t = 2.58 sec; 1) p = 10 bar; 2) 10^2; 3; 10^3; 4) $8 \cdot 10^3$; 5) 10^4; 6) 10^5; 7) 10^6; r, z, cm.

action of the REB pulse, and the energy liberation zone configuration must be recomputed. The algorithm for the solution of the problem is organized so that this recomputation is realized every time the density varies by more than 10% at some point of the zone. A conversion of the source is also provided for because of a more than 10% change in beam energy absorption in the flare.

We use a traditional hydrodynamic model to describe the dynamics of the plasma flare that occurs and of the flow of dense medium in the target at the initial stage of crater formation.

As already mentioned, the values of the plasma-flare parameters are such that it is necessary to take account of energy transfer by radiation. Trial computations showed that this transfer can be described satisfactorily in a radiant heat conduction approximation in the case of flare broadening in air of normal density. In addition, we note that because of the high optical density of the flare, energy losses by de-excitation in the surrounding space were taken into account in a surface emitter approximation by the model proposed in [7].

The strength properties of the medium start to play a substantial part in the concluding stage of crater formation in the target. To take them into account we shall start from a rigidly plastic model which results, as is shown in papers on high-velocity impact [8], in crater parameters that are in sufficiently good agreement with experiment.

Taking account of the axisymmetry of the problem, we use a cylindrical r0z coordinate system. An electron beam directed along the $\vec{0Z}$ axis is incident on a metal target of density ρ_0 located between the planes $z = -a$, $z = 0$. The space $z < -a$ and $z > 0$ is occupied by a medium with the low density ρ_1, the surrounding atmosphere. The complete system of equations describing the processes listed has the form

$$\frac{\partial \rho}{\partial t} + \operatorname{div}(\rho \vec{W}) = 0,$$

$$\frac{\partial \rho u}{\partial t} + \operatorname{div}(\rho u \vec{W}) + \frac{\partial}{dz}(p - S_{33}) - \frac{1}{r}\frac{\partial}{\partial r}(rS_{13}) = 0,$$

$$\frac{\partial \rho v}{\partial t} + \operatorname{div}(\rho v \vec{W}) + \frac{\partial}{\partial r}(p - S_{11}) - \frac{\partial}{\partial z}S_{13} + \frac{S_{22} - S_{11}}{r} = 0,$$

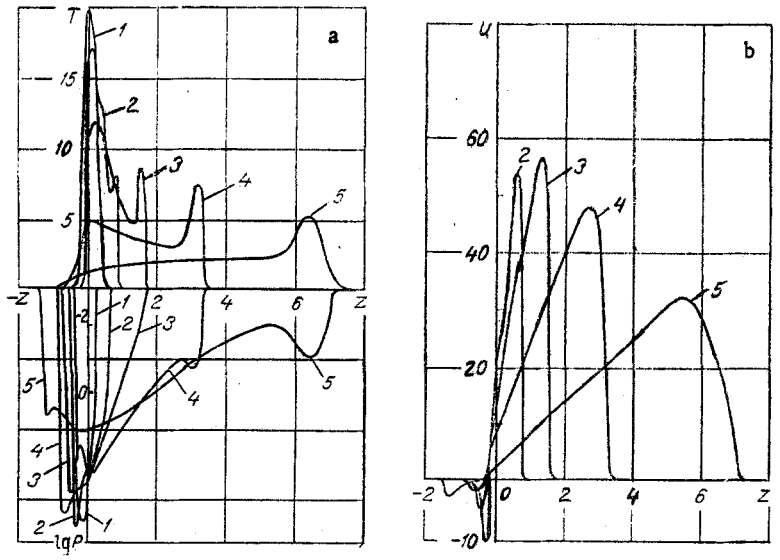

Fig. 3. Axial profiles of the pressure, temperature (a), and efflux velocity (b): 1) 0.056; 2) 0.115; 3) 0.225; 4) 0.521; 5) 1.5 μsec; T, eV; log P, kbar; z, cm.

$$\frac{\partial \rho E}{\partial t} + \operatorname{div}(\rho E \vec{W}) - \operatorname{div}(\varkappa \operatorname{grad} T) + \frac{\partial}{\partial z}((p - S_{33})u - S_{13}v) +$$

$$+ \frac{1}{r}\left(\frac{\partial}{\partial z}((p - S_{11})vr - S_{13}ur) - Q\rho + \delta L = 0,\right.$$

where δ is the delta function defined as

$$\delta = \begin{cases} 1 \text{ on the optically opaque flare surface with } T \geqslant 1 \text{ eV} \\ 0 \text{ in the whole rest of the domain.} \end{cases}$$

The equations of state for the target material [9] $\varepsilon_1 = \varepsilon(\rho, p)$ and the surrounding atmsophere [10] $\varepsilon_2 = \varepsilon(\rho, p)$ as well as the governing equation [8] describing the material properties under shear close this system of equations, where the relationship between the stress deviator and the strain rate tensor ε_{ij} can be obtained: $S_{ij} = S(\varepsilon_{ij})$.

Underlying the numerical integration of the system of equations is the method of coarse particles described in [11, 12] and extended to the case of a nonadiabatic flow and a nonregular spatial Euler mesh for the detailed resolution of the energy liberation zone itself. The computational mesh contained 80 × 50 cells along the $\overrightarrow{OZ}$ and $\overrightarrow{OR}$ axes, respectively.

Let us present certain results of a computation for the experiment conditions [2]. A REB pulse with 1-MeV electron energy acted on an aluminum plate of 1 cm thickness. The duration of the 140-kA current pulse was 100 nsec, the beam radius was 0.1 cm, and the energy in the beam 14 kJ. Integrated characteristics of the REB interaction with the target are shown in Fig. 1. All the energy characteristics are normalized by the total energy liberated in the region under consideration. It is seen that about 70% of the beam energy is absorbed by the target to the end of the action by the pulse, where 60% of this energy is in its thermal component. The mean coefficient of electron energy reflection was 10%. After termination of the pulse action, a further development of the plasma flare occurs because of the target rupture products. At the end of the computation 35% of the beam energy was the kinetic energy fraction. It is seen in the graph of the crater depth growth (curves 5 and 6) that up to 0.7 μsec the crater starts to be formed from the rear side of the slab also, which is related to unloading of the material after the emergence of the shock on the interface of the media. The specific mass ejection M/E from the crater reached a magnitude of 100 μg/J to the end of the computation. The specific impulse of the emission grew almost linearly with time and reached 15 dyne·sec/J at the end of the computation.

Presented in Fig. 2 are isobars of the process for t = 0.115 μsec and t = 2.5 μsec in r0z space, and appropriate target hole profiles are also shown. Let us note that in the intensive interaction phase t ≤ 100 nsec, the pressure in the action zone reached 8.9 Mbar, the temperature 19 eV, and the compression (ρ/ρ_0) 1.455.

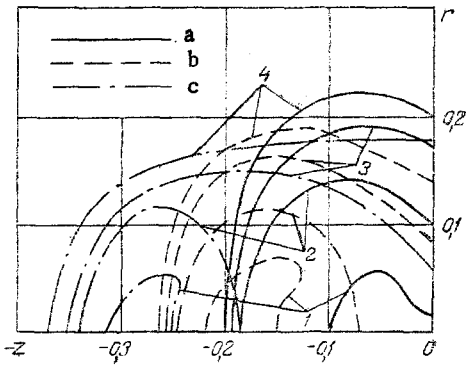

Fig. 4. Dynamics of the energy liberation zone shape: a) t = 0.022 μsec; b) 0.066 μsec; c) 0.1 μsec; 1) 100 MeV/electron·g; 2) 10; 3) 1; 4) 0.1.

Distributions of the pressure, temperature, and efflux velocity along the axis of symmetry $\vec{OZ}$ are reprsented in Fig. 3 for different times. The characteristic features of bulk energy liberation in a target during the action of a pulse are seen (curves 1, 2, and 3), being apparent in that the maximal temperature on the order of 20 eV is reached in the target at a distance of 0.24 cm from the surface where the rupture products density is large and the main energy liberation occurs.

The dynamics of energy liberation zone formation is displayed in Fig. 4, where the times 0.022, 0.066, and 0.1 μsec are represented. As the substance is ejected from the interaction zone, the maximum energy liberation shifts into the target bulk, while the angular scattering diminishes. Later, after termination of the pulse action, a plasma flare with maximum temperature develops intensively on the shock front, as is also customary. The shock propagates over the target substance, resulting in fragment formation on the rear side. The spall products have a relatively low 0.05 eV temperature and a velocity on the order of 3 km/sec up to the formation of the through hole. The velocity of the flare vapor here reaches 30 km/sec on the front.

The data presented show that the theoretical model described for charged-particle high-current beam interaction with a metallic obstacle correctly reflects the fundamental regularities of the interaction process and is in sufficiently good agreement with experimental results.

NOTATION

t, time; z, r, axial and radial coordinates; ρ, density; u, v, axial and radial components of the velocity $\vec{W}$; E, total specific energy; p, pressure; S_{ij}, stress deviator; Q(z, r, t), energy liberated by the source per unit mass of substance in unit time; L, energy loss due to surface deexcitation; $\varkappa = 5.3\,\sigma T^3 l_R$, coefficient of radiant heat conduction; l_R, mean, Rosseland-averaged, radiation path; $\sigma = 5.67 \cdot 10^{-5}$ erg/cm²·deg⁴.

LITERATURE CITED

1. I. P. Afonin, M. V. Babykin, B. V. Baev, et al., "Focusing of a powerful beam in a diode and target exposure in the 'Angara-1' installation," Reports to an All-Union Conf. on Engineering Problems of Thermonuclear Reactors. Proceedings of a Congress [in Russian], Vol. 2, VNII ÉFA, Leningrad (1977), pp. 104-113.
2. M. V. Babykin, "Electronic thermonuclear synthesis," Science and Engineering Surveys. Plasma Physics [in Russian], Vol. 1, Pt. 2, VINITI, Moscow (1981), pp. 5-80.
3. G. S. Romanov and M. V. Suzdenkov, "Dynamics of crater formation under the effect of high-current charged-particle beams on a metal obstacle," Dokl. Akad. Nauk BSSR, 26, 496-499 (1982).
4. M. M. Widner and S. L. Thompson, "Calculation of anode witness plate damage due to pinched relativistic electron beams," Sandia Report, Sand-74-351 (1974).
5. A. F. Akkerman, Yu. M. Nikitushev, and V. A. Botvin, Solution of Fast Electron Transport Problems in a Substance by the Monte Carlo Method [in Russian], Nauka, Alma-Ata (1972).
6. B. V. Alekseev, V. I. Ivanov, and L. I. Rudakov, "Numerical investigation of relativistic electron beam interaction with targets," Zh. Tekh. Fiz., 47, No. 3, 504-509 (1977).
7. G. L. Broud, Effect of a Nuclear Explosion [Russian translation], Mir, Moscow (1971).
8. D. Deans and D. Walsh, "Theory of impact," in: High-Velocity Shock Phenomena [Russian translation], Mir, Moscow (1973), pp. 48-111.

9. L. V. Al'tshuler, A. V. Bushman, M. V. Zhernokletov, et al., "Unloading isentropes and equations of state of metals for high energy densities," Zh. Eksp. Teor. Fiz., 78, No. 2, 741-760 (1980).
10. F. N. Borovic, M. A. Elyashevich, et al., "Optical properties of aluminum plasma," Proc. 15th Int. Conf. on Phenomena in Ionized Gases, Part 2, Minsk (1981), pp. 911-912.
11. O. M. Belotserkovskii and Yu. M. Davydov, "Nonstationary coarse particle method for gasdynamic computations," Zh. Vychisl. Mat. Mat. Fiz., 11, No. 1, 182-207 (1971).
12. G. S. Romanov, M. V. Suzdenkov, and A. V. Teterev, "On the accuracy of the method of coarse particles for gasdynamic problems," Zh. Vychisl. Mat. Mat. Fiz., 21, No. 3, 798-803 (1981).

THERMAL PROPERTIES OF AN AQUEOUS SOLUTION OF SODIUM CHLORIDE AT A CONCENTRATION OF 200 g/liter

T. S. Akhundov and M. V. Imanova

UDC 531.756

Results are offered from a study of density and vapor tension of an aqueous solution of sodium chloride at temperatures of 598.15°K and pressures to 40 MPa.

The experimental values of density and vapor tension of an aqueous solution of sodium chloride containing 200 g salt per liter of solution were obtained by the constant-volume piezometer method. The pressure was measured by load piston manometers, types MP-600 and MP-60, with 0.05% accuracy, and the temperature was determined by a reference platinum resistance thermometer with uncertainty of ±0.02°.

The total relative uncertainty in density determinations did not exceed ±0.1%.

The experimental data are presented in Table 1. Also shown are measured values of vapor tension and densities of the saturated liquid at temperatures of 373.15-598.15°K (last column), obtained by graphic extrapolation of the isotherms to the corresponding saturation pressures.

The vapor tension of sodium chloride P_s (MPa) for concentrations of C = 0-300 g/liter is described by the equation

$$P_s = P_w \cdot 10^{-1.77975 \cdot 10^{-4} \cdot C^{1.1}}.$$

This equation generalizes the experimental data with an error no greater than ±0.2%.

NOTATION

P, pressure, MPa; T, temperature, °K; ρ, liquid density, kg/m³; P_s, saturated vapor pressure of solution, MPa; P_w, saturated pressure of water vapor, MPa; C, solution concentration, g/liter; $v = -1.77975 \cdot 10^{-4}$, coefficient.

M. Azizbekov Institute of Petroleum and Chemistry, Baku. Translated from Inzhenerno-Fizicheskii Zhurnal, Vol. 47, No. 6, pp. 957-959, December, 1984. Original article submitted September 30, 1983.

0022-0841/84/4706-1437$08.50